

University of New Orleans
ScholarWorks@UNO

University of New Orleans Theses and
Dissertations

Dissertations and Theses

Fall 12-20-2018

Automating the Detection of Precipitation and Wind Characteristics in Navy Ocean Acoustic Data

Joseph T. Kuhner
University of New Orleans, joseph.kuhner@gmail.com

Follow this and additional works at: <https://scholarworks.uno.edu/td>

Recommended Citation

Kuhner, Joseph T., "Automating the Detection of Precipitation and Wind Characteristics in Navy Ocean Acoustic Data" (2018). *University of New Orleans Theses and Dissertations*. 2567.
<https://scholarworks.uno.edu/td/2567>

This Thesis is protected by copyright and/or related rights. It has been brought to you by ScholarWorks@UNO with permission from the rights-holder(s). You are free to use this Thesis in any way that is permitted by the copyright and related rights legislation that applies to your use. For other uses you need to obtain permission from the rights-holder(s) directly, unless additional rights are indicated by a Creative Commons license in the record and/or on the work itself.

This Thesis has been accepted for inclusion in University of New Orleans Theses and Dissertations by an authorized administrator of ScholarWorks@UNO. For more information, please contact scholarworks@uno.edu.

Automating the Detection of Precipitation and Wind Characteristics in Navy Ocean Acoustic
Data

A Thesis

Submitted to the Graduate Faculty of the
University of New Orleans
In partial fulfillment of the
Requirements for the degree of

Master of Science
in
Applied Physics

By

Joseph Kuhner

B.S. Saint Mary's College, 2004
M.S. University of Southern Mississippi, 2011

December, 2018

Contents

- List of Figures iii
- Abstract..... iv
- Introduction 1
- Sensors, Sources, and Data..... 2
 - Acoustics 2
 - Precipitation..... 2
 - Sea State 2
- Precipitation Signatures..... 4
- Precipitation Detection Automation 7
- Determination of Minimum Threshold 9
- Sea State and Wind Speed..... 12
- Wind Detection and Automation 14
- Test Event 1..... 16
- Test Event 2..... 18
- Test Event 3..... 20
- Conclusions 22
- Bibliography 23
- Vita 24

List of Figures

Fig. 1 Spectrogram record of a precipitation event. Color scale is in dB.	5
Fig. 2 Buildup (Green), Peak (Red), and Falloff (Blue) of precipitation event.	5
Fig. 3 Observed precipitation events with associated in-situ weather observation.	6
Fig. 4 Precipitation curve with identified maximum and minimum frequency levels.	7
Fig. 5 Results of linear regression between minimum and maximum frequency levels	8
Fig. 6 Slope ratio comparison of a rain event (left) and non-rain event (right).	8
Fig. 7 Noise Level distribution at 20 kHz (left) and Slope Ratio Distribution (right).	9
Fig. 8 Low pass filtered distribution curve with applied 1st order derivative to isolate peaks.	10
Fig. 9 Results of Gaussian Mixture Model applied to slope ratio.	10
Fig. 10 Noise level distribution derived from the positive slope ratio distribution.	11
Fig. 11 Comparison of modeled wave height and winds speeds. Poly lines represent trends.	12
Fig. 12 Truncated version of the Beaufort scale for Wind Speed and Wave Height.	13
Fig. 13 Scatter plot of wave height and noise level at 5000 Hz.	14
Fig. 14 Truncated Beaufort Scale	15
Fig. 15 Test Event 1, light rain with moderate wind speed.	16
Fig. 16 Results for precipitation automation.	17
Fig. 17 Results for wind category.	17
Fig. 18 Test Event 2, moderate/heavy rain with moderate/rough wind speed.	18
Fig. 19 Results for precipitation automation.	19
Fig. 20 Results for wind category.	19
Fig. 21 Test Event 3, light rain with moderate wind speed.	20
Fig. 22 Results for precipitation automation.	21
Fig. 23 Results for wind category.	21

Abstract

A challenge in Underwater Acoustics is identifying the independent variables associated with an environment's ambient noise. A strict definition of ambient noise would focus on non-transient signatures and exclude transient impacts from marine mammals, pelagic fish species, man-made sources, or weather events such as precipitation or wind speeds. Recognizing transient signatures in acoustic spectra is an essential element for providing environmental intelligence to the U.S. Navy, specifically the acoustic signatures from meteorological events. While weather event detection in acoustic spectra has been shown in previous studies, leveraging these concepts via U.S. Navy assets is largely an unknown. Environmental intelligence collection can be improved by detecting precipitation events and establishing wind velocities with acoustic signatures. This will further improve meteorological models by enabling validation from both manned and unmanned sub-surface assets.

Keywords: Acoustics, Spectra, Precipitation, Wind, Model, Detection, Automation, Noise, Navy, Meteorology, Weather

Introduction

Noise spectra collected with stationary hydrophones can detect the presence of rain and estimate wind speeds. During the 2012 and 2016 NASA Salinity Processes in the Upper Ocean Regional Study field experiments, recordings from a Passive Aquatic Listener were used in a numerical procedure to classify precipitation and wind velocities [1]. In 2005, the Applied Physics Laboratory from the University of Washington developed a technique to determine precipitation presence and rainfall-rate from buoy positioned hydrophones [2]. In both cases, acoustic signatures within the spectrogram were observed with the presence of rainfall and excessive winds. This study builds a process that both detects precipitation events and categorizes wind velocities with U.S. Navy collected ambient noise data. In contrast to other studies, the U.S. Navy uses constantly moving passive listening devices that can migrate both horizontally and vertically through the water column. By integrating signal processing and statistical modeling techniques, an algorithm can automate the detection of precipitation and wind velocities within a spectrogram. The timescale of the collected ambient noise data encompasses multiple weeks of continuously measured noise levels from frequencies between 1 and 40 kHz. Validation is accomplished through in-situ observations, historical model derived weather conditions, and historical satellite imagery.

Sensors, Sources, and Data

Acoustics

The passive acoustic sensors used in this study collect 1 minute averages of frequencies between 1 and 40 kHz. Data were collected continuously over month long timelines. Since the sensors are not stationary, data quality is commonly degraded due to transient noise associated with speed (flow noise) and transmission loss due to excessive sensor depth.

Precipitation

Rain rate is collected through the PERSIANN-CCS (Precipitation Estimation from Remotely Sensed Information using Artificial Neural Networks – Cloud Classification System) [3] developed by the University of California, Irvine. PERSIANN-CCS uses a variable threshold cloud segmentation algorithm which enables the identification and separation of individual patches of clouds. These patches can be classified based on texture, geometric properties, dynamic evolution, and cloud top height. Classifications are used to assign rainfall values to pixels within each cloud based on the relationship between rain-rate and brightness temperature. PERSIANN-CCS provides a real time high resolution (4 km x 4 km) precipitation product.

Sea State

Wind speed and wave height measurements used for category validation and model correlation were collected by the National Data Buoy Center using a Self-Contained Ocean Observation Payload (SCOOP) [4]. Observations were gathered throughout 2013 in the mid-Gulf of Mexico. Recorded values are averaged over a 40 minute window with accuracies of +/- 1.0 m/s and +/- 0.2 m respectively. Range values for wind speed and wave height are 0 to 62 m/s and 0 to

35 m. Model data used for significant wave height tabulation were collected from the Simulating Waves Nearshore (SWAN) model [5]. The Coupled Ocean/Atmosphere Mesoscale Prediction System (COAMPS) [6] developed by the Naval Research Laboratory (NRL) was used for wind forecast. COAMPS is a numerical model with a spatial resolution of 4 km.

Precipitation Signatures

Rain generated sound materializes from two physical occurrences: the impact of the raindrop on the ocean surface and the bubble that gets trapped beneath the surface from the splash. The noise level is dependent on raindrop size, rainfall rate, and in some cases wind speed. Increased wind speeds have been shown to impact the location of the peak frequency in the spectra [7]. In cases of large raindrop sizes (diameter >3.5 mm) and heavy rainfall (>20 mm/hour), the noise level is mostly generated by the impact of the raindrop and has little dependence on wind speed [2]. Researchers have been able to identify characteristics of precipitation in acoustic spectra that differentiate the signals from ambient noise. This study will use spectral shape and noise level to isolate precipitation in acoustic signals.

Fig. 1 illustrates a spectrogram record of a precipitation event. This event is consistent with a light precipitation event in a low wind environment [8]. The peak frequency is between 13 and 15 kHz, the sound level is characteristic of a rainfall rate between 2 and 5 mm/hour with a rain drop diameter between 0.8-1.2 mm. In Fig. 2, a spectra time series of the precipitation event quantifies the spectra changes as the event passes the acoustic sensors. While the maximum noise level changes, the peak frequency remains consistent at 15 kHz.

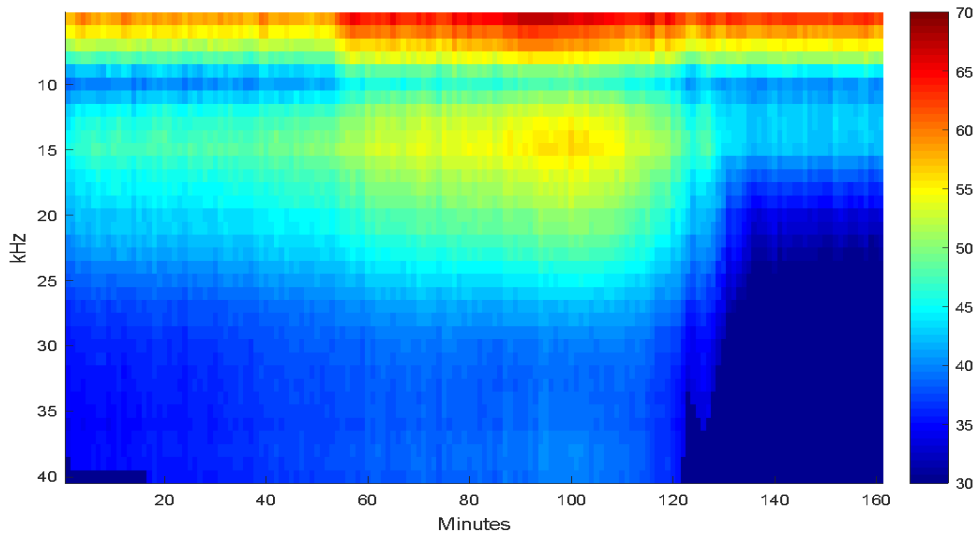


Fig. 1 Spectrogram record of a precipitation event. Color scale is in dB.

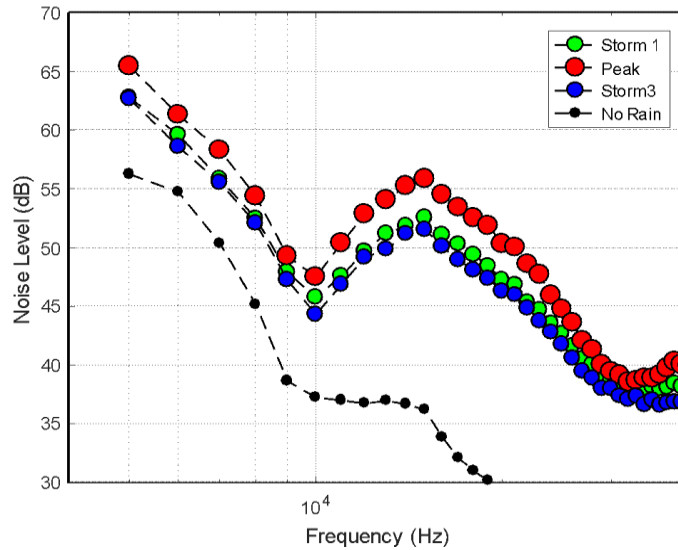


Fig. 2 Buildup (Green), Peak (Red), and Falloff (Blue) of precipitation event.

During a precipitation event, the noise spectra will display a feature similar to a 2nd order curve between approximately 10 and 20 kHz. While the overall noise level will usually correlate to the amount of rainfall, an important variable is the distance of the sensor from the event. Using acoustic modeling of transmission loss, signals at a frequency of 15 kHz can attenuate by as much as 60 dB loss over a horizontal distance of 1 kilometer and a vertical

distance attenuation as high as 45 dB at a depth of only 100 feet. With this information, it can be assumed that precipitation signals in the noise spectra must be associated with relatively local precipitation events.

Fig. 3 offers the amalgamation of multiple observed precipitation events to illustrate the presence of the 2nd order curve. Each curve is associated with an in-situ observation of observed rainfall and wind speed. Rainfall is separated into three user observed categories; Light, Moderate, and Heavy (it should be noted that these categories do not represent an objective measure). While these categories have no official numerical representation, the ordering appears consistent with noise levels associated with the recorded rainfall category. As mentioned, the location of frequency peaks and curve shape are susceptible to multiple dependent variables including rainfall rate, wind speed, and other environmental irregularities. The curve shape appears to be a consistent indicator of precipitation.

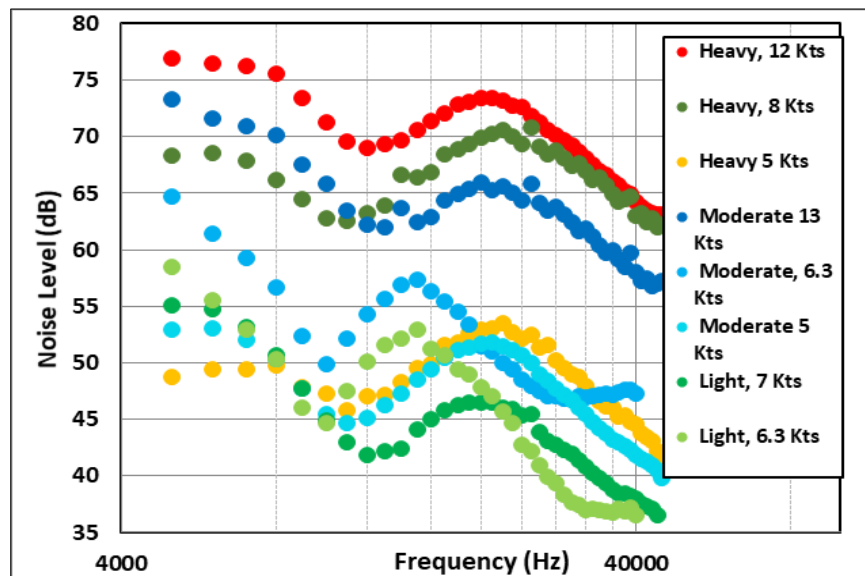


Fig. 3 Observed precipitation events with associated in-situ weather observation.

Precipitation Detection Automation

The detection of precipitation is based on two characteristics: quantifying the presence of the 2nd order curve and estimating the value of the peak noise level. To identify the curve, a simple linear regression technique is used based on minimum and maximum noise levels between 10 kHz and 20 kHz. Fig. 4 illustrates a validated precipitation curve with the minimum and maximum noise levels identified. Calculating the linear regression of the values between the identified minimum and maximum will model the slope of the curve, as shown by the blue line in Fig. 5. The modeled slope can be correlated to a single value which will be referred to as the slope ratio. Uncontaminated noise spectra that exhibit a positive rain ratio satisfy the first characteristic for the detection of precipitation.

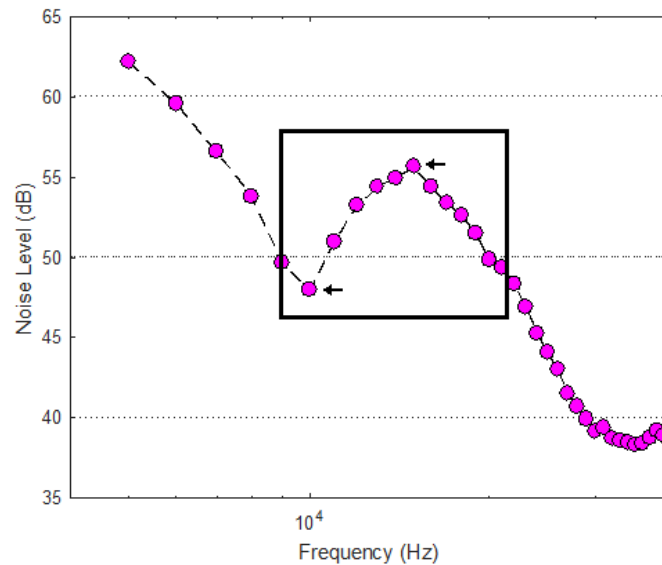


Fig. 4 Precipitation curve with identified maximum and minimum frequency levels.

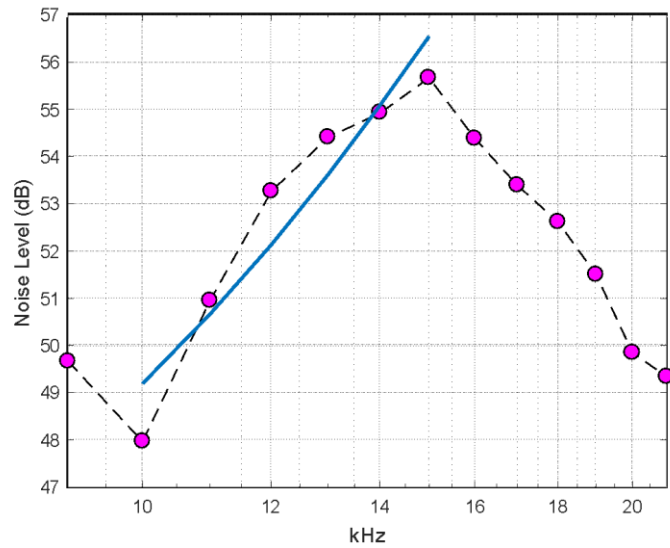


Fig. 5 Results of linear regression between minimum and maximum frequency levels

Fig. 6 illustrates two spectra and associated slope values, showing the positive value for the precipitation event and the negative value for the rainless event.

A minimum noise level threshold was determined by amalgamating the slope ratio for an entire continuously collected dataset. A combination of in-situ observations and satellite derived rainfall rates were used to identify the presence of precipitation events within the dataset. For the purposes of this research, a minimum threshold is the only necessary element for detection.

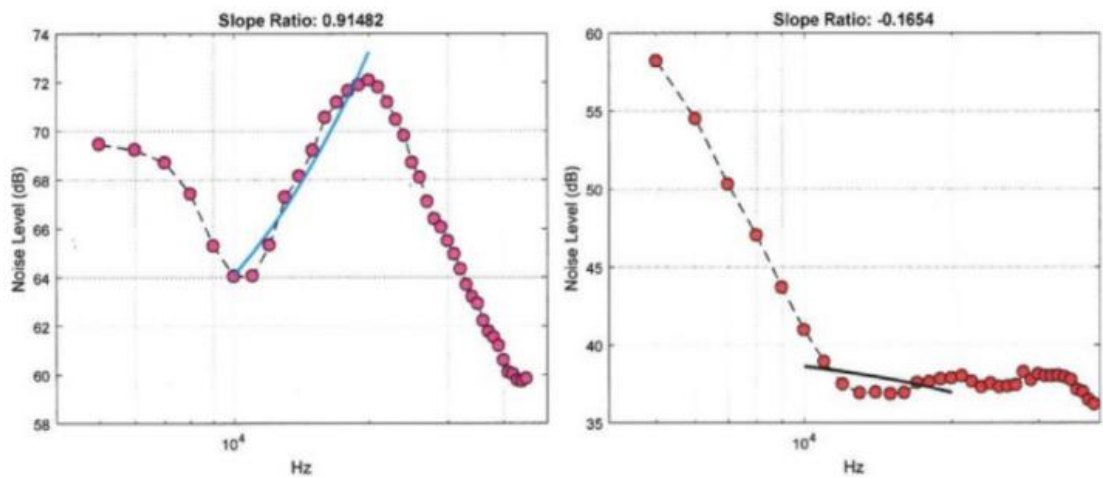


Fig. 6 Slope ratio comparison of a rain event (left) and non-rain event (right).

Determination of Minimum Threshold

Making an accurate assessment for a minimum precipitation threshold requires examining the distributions (histograms) for noise level and slope ratio, Fig. 7.

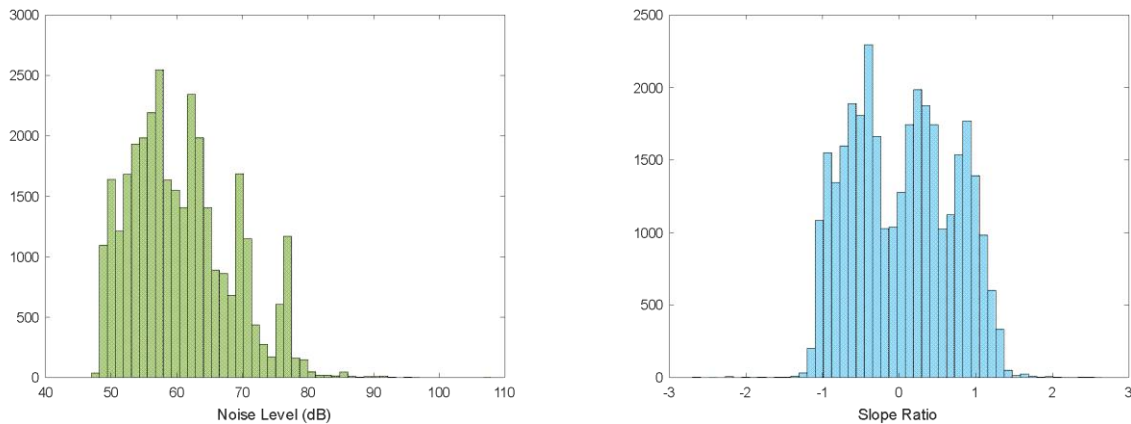


Fig. 7 Noise Level distribution at 20 kHz (left) and Slope Ratio Distribution (right).

The noise level distribution displays characteristics of a log-normal distribution and the slope ratio distribution is clearly multimodal. The goal will be to isolate the distributions associated with slope ratio, specifically with respect to positive slope values that represent a precipitation signature. This isolation can be done by using a one dimensional Gaussian Mixture Model (GMM). The GMM is a three step process used to assign probabilities to points in a multimodal distribution based on initial estimates for modal size (number of distributions in the multimodal distribution), means, variances, and probabilities. After the initialization step, an expectation and maximization step are utilized to recalculate mean, variance, and probability in an attempt to accurately define each distribution in the multimodal distribution. For the purposes of this study, the modal size and mean will be determined through a 1st order derivative from the distribution curve calculated using a moving average. The derivative is able to identify local maxima within the smoothed curve, Fig 8.

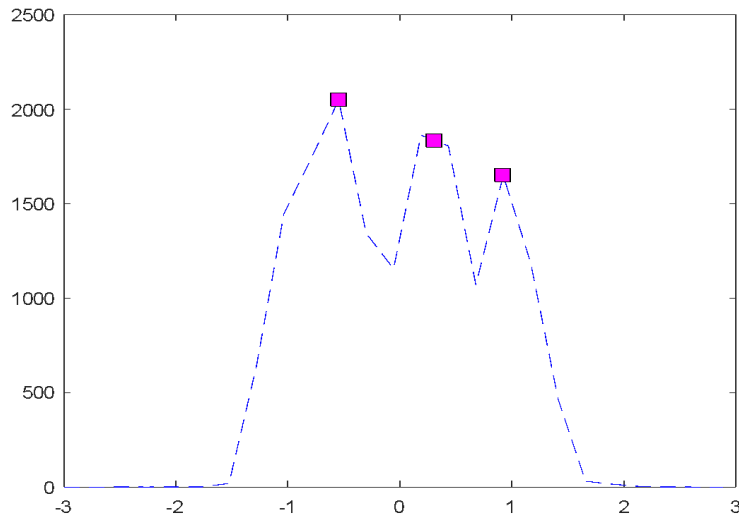


Fig. 8 Low pass filtered distribution curve with applied 1st order derivative to isolate peaks.

The number of identified peaks represent the number of distributions and the x-axis values represents the means. Using these values in the initialization step yields the results in Fig. 9.

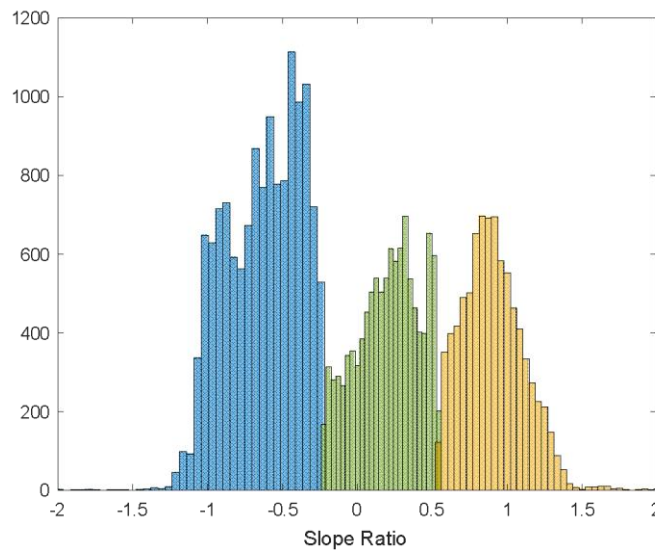


Fig. 9 Results of Gaussian Mixture Model applied to slope ratio.

The distributions in Fig. 9 can be categorized as negative (blue), neutral (green) and positive (yellow). The focus of analysis will be on the data points within the positive distribution. Associating these points with their representatives in the noise level distribution produces the result in Fig. 10.

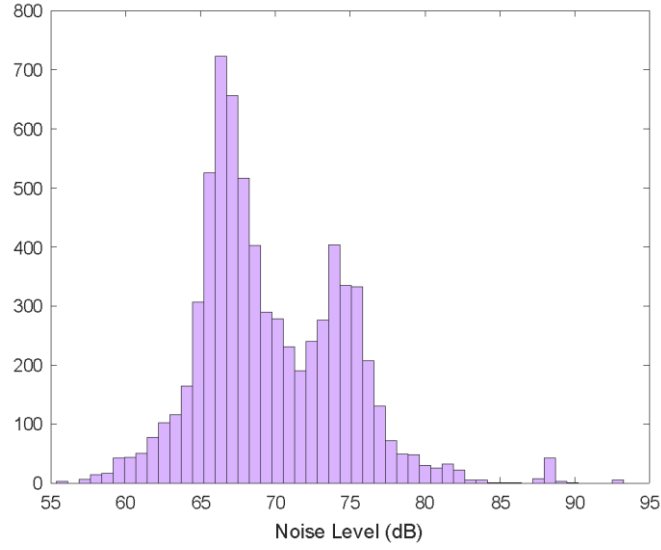


Fig. 10 Noise level distribution derived from the positive slope ratio distribution.

The distribution from Fig. 10 indicates two periods of varying rainfall caused by moderate and heavy precipitation. This was verified using PERSIANN-CCS data that estimated rates between 2-132 mm/hour rainfall. The 1st percentile from this distribution will be used as the minimum threshold for rain detection.

Sea State and Wind Speed

Correlating an acoustic signature to wind speed can be a challenge since the noise is actually caused by wind generated breaking waves. Wave heights and periods vary with wind speed, time, and fetch. Fig. 11 shows a modeled time series comparison to illustrate the relationship between wave height and wind speed. Trends within the modeled variables tend to follow a similar pattern. What should be immediately noticeable is the time lag between increased wind speeds and wave height. Also, increases in wind speed may not be apparent in the wave heights due to the time period of peak intensities.

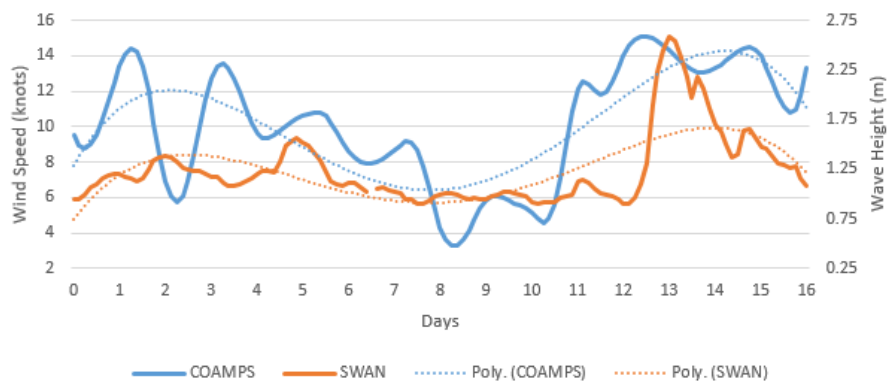


Fig. 11 Comparison of modeled wave height and winds speeds. Poly lines represent trends.

Wave heights derived via satellite imagery calculate significant wave height over a surface area. This is a similar process to sea state descriptions used for observed effects on water. In both cases, wave heights are used to quantify a given area's sea conditions. This concept of estimating winds speeds from wave heights is utilized through the Beaufort scale. Using visual observations and numerical analysis, Sir Francis Beaufort developed a scale to link sea state with wind speed. The resolution of the Beaufort scale is higher than necessary for the purposes of this study. Instead of the thirteen categories commonly used in the Beaufort scale, a truncated version of the scale will be used consisting of four categories given in Fig. 12.

Validating the truncated scale can be done by using a time series of NOAA buoy collected wind speeds and wave heights from the Gulf of Mexico. Comparing the associated truncated scale values shows the agreement between wind and wave categories occurs 82% of the time. The majority of disagreements occurred with values within 10% of the set threshold. Using these threshold values, it can be reasonably assumed that wave height can be used as a predictor of wind speed.

From sea state, a category for wind speed can be determined using the truncated scale.

Truncated Scale	Wind Speed (knots)	Wave Height (m)
CAT I (Calm)	0 – 10	0 – 0.5
CAT II (Light)	11 – 16	0.5 – 1.25
CAT III (Moderate)	17 – 21	1.25-2.5
CAT IV (Rough)	>21	>2.5

Fig. 12 Truncated version of the Beaufort scale for Wind Speed and Wave Height.

Wind Detection and Automation

In order to extrapolate wind speed, historical modeled wave heights were used to correlate the acoustic signature to sea state. Calculating a linear regression of the relationship between wave height and the noise level at 5000 Hz produced a result similar to the “Knudsen Curves” [9] and results published by Murugam, Natarajin, and Kumar [10]. The exact results are shown in Fig. 13.

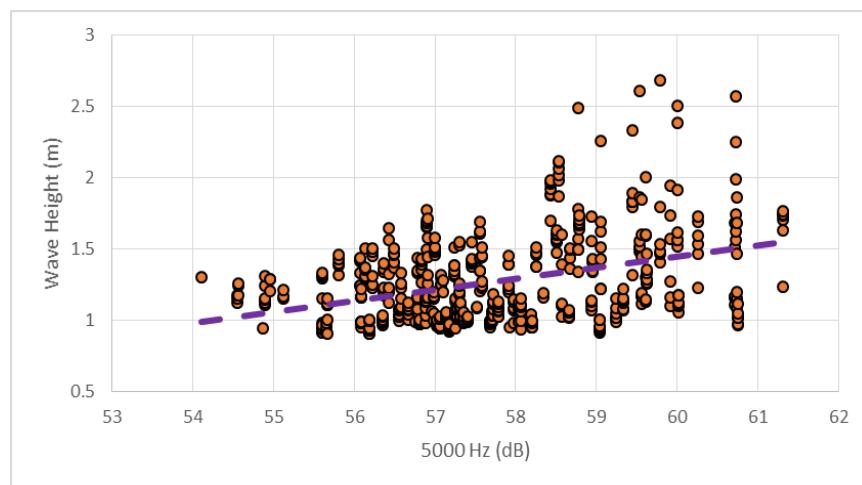


Fig. 13 Scatter plot of wave height and noise level at 5000 Hz.

Connecting the truncated scale wave height with associated noise values at 5000 Hz produces the table in Fig. 14. When using the table, it is strongly encouraged to use a time span comparison value as opposed to an instantaneous value.

Results from the SWAN data with the truncated categories using a 5000 Hz noise level show approximately 80% agreement. Thus, using the above table should merit acceptable results for wind speed derivation from observed noise. The specific automation process utilizes a Savitzky-Golay filter as a representation of a time series for the noise level comparison value.

Category	Wind Speed (knots)	Noise Level (dB 5KHz)
I	0 – 10	0 - 48
II	11 – 16	49 - 58
III	17 – 21	59 - 74
IV	>21	>74

Fig. 14 Truncated Beaufort Scale

Test Event 1

This event was recorded as having light precipitation associated with moderate winds. Satellite imagery confirmed 1-2 mm/hour rainfall and COAMPS wind speeds were consistent with categories 2 (Light) and 3 (Moderate). The spectrogram for this event is captured in Fig. 15, the color scale is in dB.

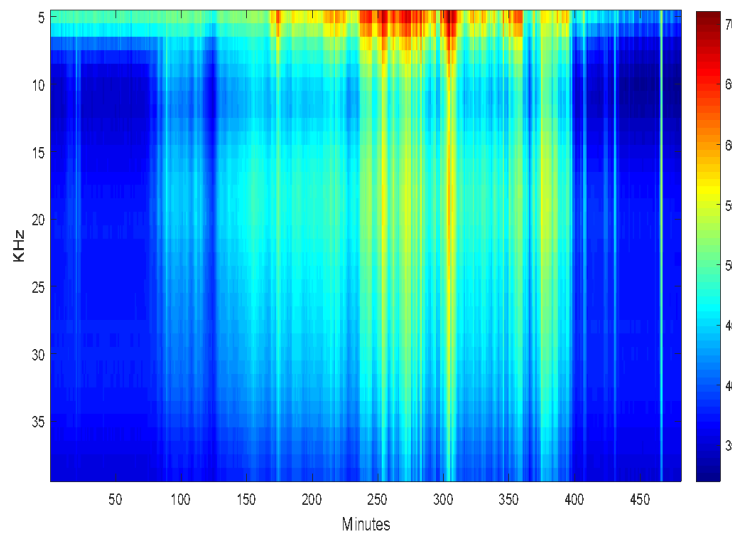


Fig. 15 Test Event 1, light rain with moderate wind speed.

Applying the techniques for precipitation and wind produces the results shown in Fig. 16 for rain noise level and Fig. 17 for wind category determination. The mean noise level for rain fall is consistent with a light precipitation event and the wind evaluation shows predominantly light and moderate wind speeds.

In this case, in-situ observations were accurate. However, this isn't always the case.

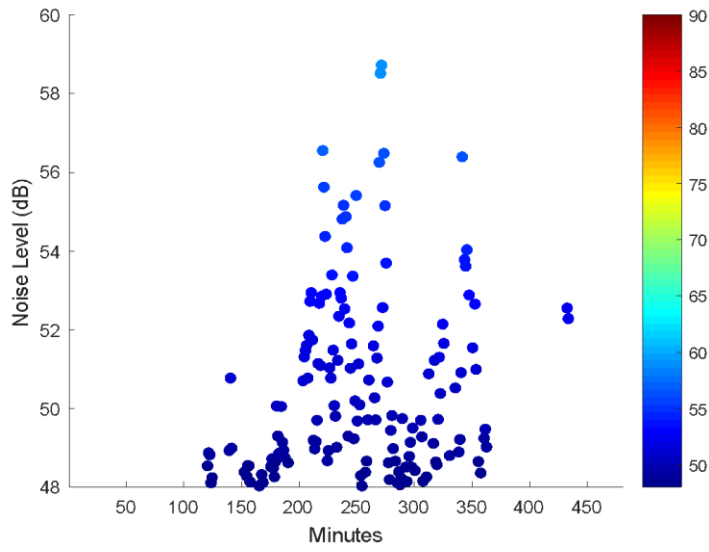


Fig. 16 Results for precipitation automation.

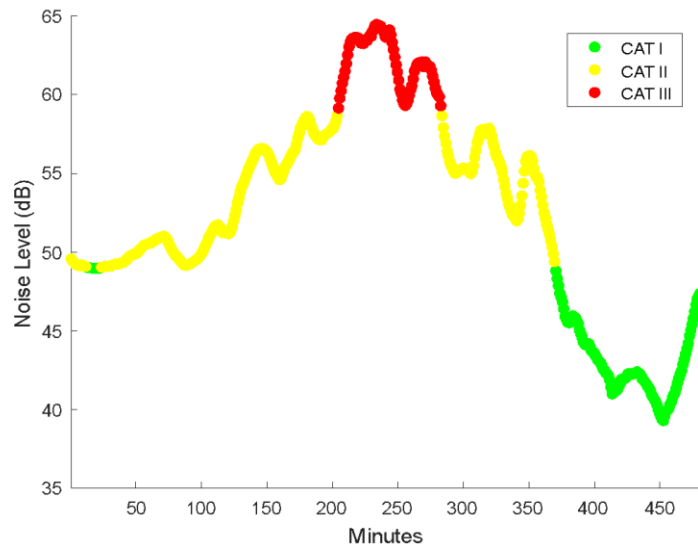


Fig. 17 Results for wind category.

Test Event 2

An observer of this event categorized the rain as moderate and the wind as light. The satellite imagery and COAMPS tell a different story with a rain fall rate of 131 mm/hour and winds in the moderate/rough range. After researching the date and location, it was determined the sensors captured the acoustics signatures of a tropical storm. The spectrogram for this event is displayed in Fig. 18, color scale is in dB.

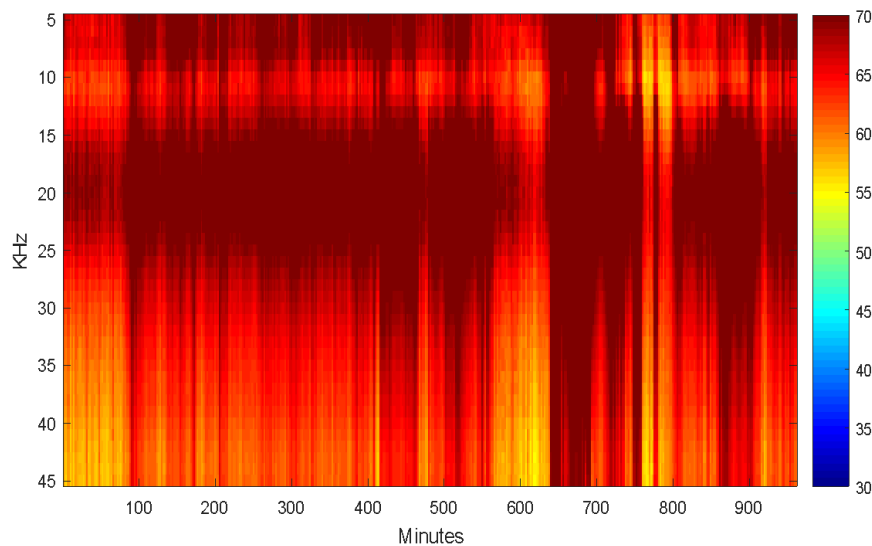


Fig. 18 Test Event 2, moderate/heavy rain with moderate/rough wind speed.

The automation detected moderate and heavy rain signatures with moderate and rough wind speeds. While the visual observation didn't necessarily support the findings, the combination of supporting satellite and model data depict a different weather picture. Fig. 19 and Fig. 20 shows the graphical results of the automation.

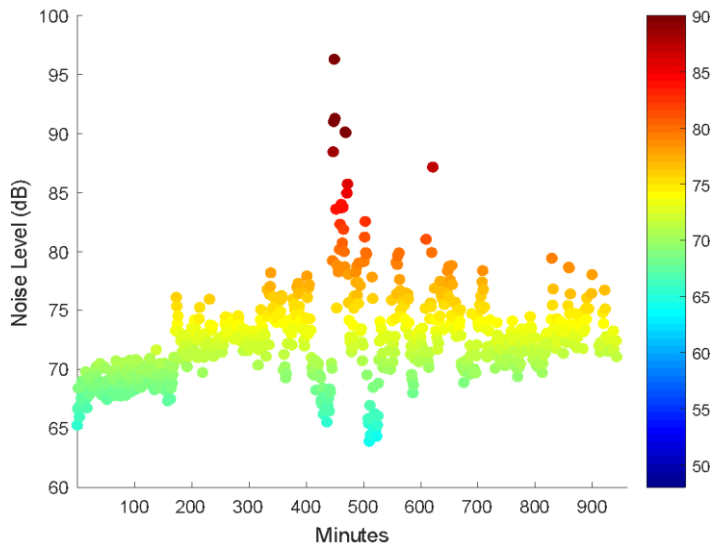


Fig. 19 Results for precipitation automation.

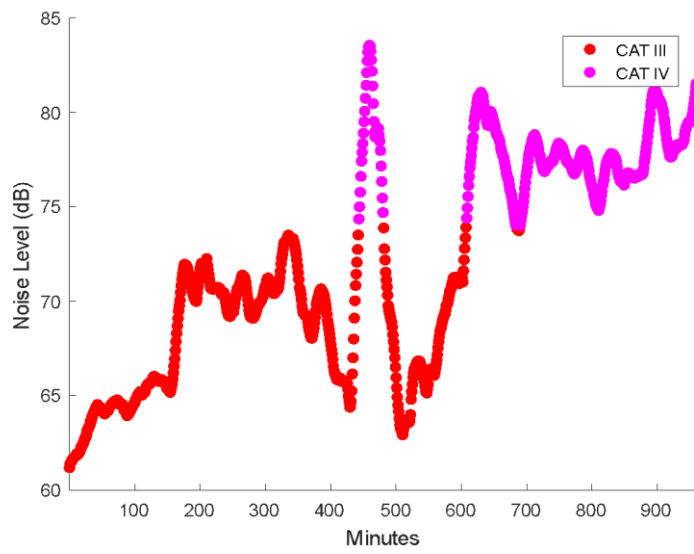


Fig. 20 Results for wind category.

Test Event 3

Satellite imagery confirmed 0-1 mm/hour rainfall and COAMPS wind speeds were in the category 3 range throughout the duration of the event. Observers described this event in a similar description to the derived satellite and model findings. While a peak in activity is easily seen around the 110 minute mark, the precipitation signatures capture an increase and an eventual cessation of rainfall. The spectrogram for this event is captured in Fig. 21.

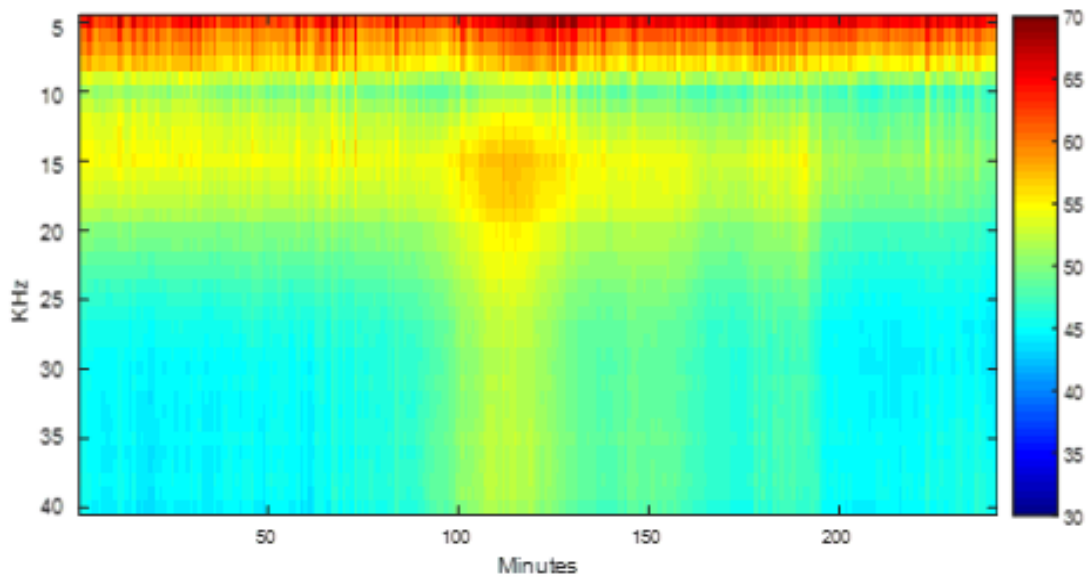


Fig. 21 Test Event 3, light rain with moderate wind speed.

Automation was largely in agreement with in-situ observations and validation datasets. Results showed both light precipitation and moderate level wind speeds. Fig. 22 and Fig. 23 show the graphical results of the computer analysis.

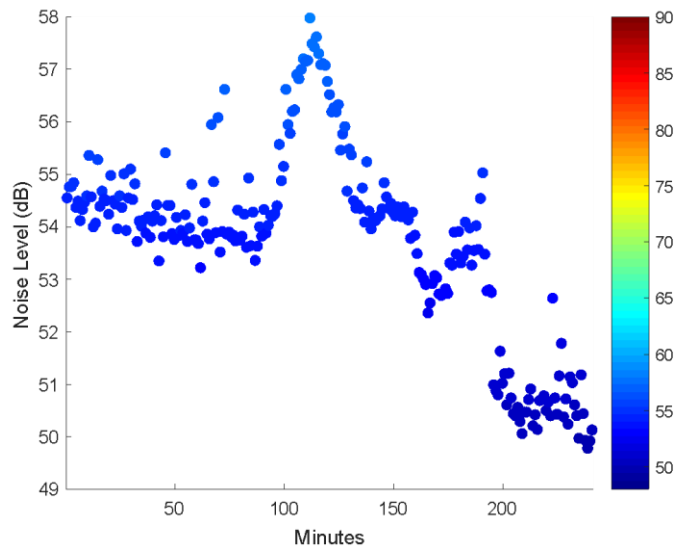


Fig. 22 Results for precipitation automation.

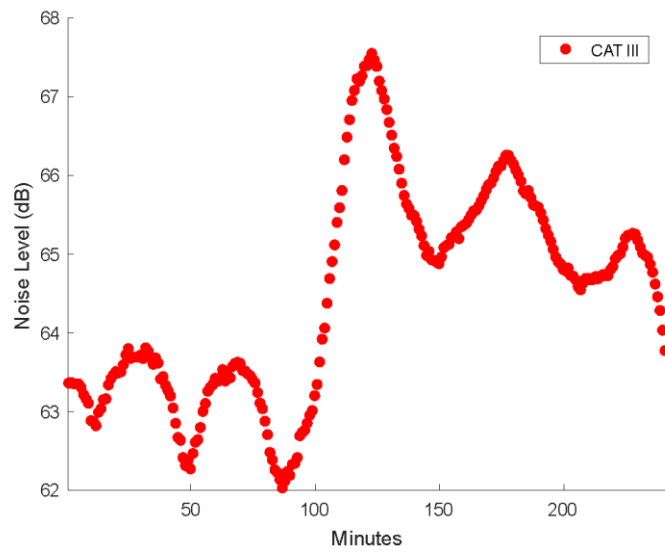


Fig. 23 Results for wind category.

Conclusions

There are several variables necessary to accurately characterize meteorological conditions associated with precipitation and wave/wind interaction with ambient noise. It appears likely that the described methodology from this research can provide valuable environmental intelligence to U.S. Navy assets. Previous reliance on subjective human observations can be replaced with an objective measure. While the categorical measures of intensity used with this study lack refinement, temporal references associated with period lengths of storm and wind activity can be useful for defining climatological descriptions associated with an area of interest. While this study focused on simply detection, correlating noise level or slope ratio to the amount of rainfall appears to be a logical next step.

Bibliography

- [1] SPURS-2 Planning Group. 2015. From salty to fresh – Salinity Processes in the upper-ocean Regional Study-2 (SPURS-2): Diagnosing the physics of a rainfall-dominated salinity minimum. *Oceanography* 28(1): 150-159, <https://doi.org/10.5670/oceanog.2015.15>.
- [2] Jeffery A Nystuen, “Rainfall measurements using underwater ambient noise,” in Acoustical Society of America, 1986, pp. 972-982.
- [3] Center for Hydrometeorology and Remote Sensing, PERSIANN – Cloud Classification System (CCS), <http://chrsdata.eng.uci.edu>
- [4] National Data Buoy Center, ‘What are the sensors’ reporting, sampling, and accuracy readings?’, <https://www.ndbc.noaa.gov/ras.shtml>
- [5] The SWAN Team, 2010: User Manual SWAN Cycle III Version 40.81, http://swanmodel.sourceforge.net/online_docs/swanuse/swanuse.html
- [6] COAMPS Model, ‘The Coupled Ocean/Atmosphere Mesoscale Prediction System (COAMPS)’, <https://www.cencoos.org/data/models/coamps>
- [7] J. Scrimger, D. Evans, G. McBean, D. Farmer, and B. Kerman, “Underwater noise due to rain, hail, snow,” in Acoustical Society of America, 1987, pp. 79-86.
- [8] Barry B. Ma, Jeffery A. Nystuen, and Ren-Chieh Lien, “Prediction of underwater sound levels from rain and wind,” in Acoustical Society of America, 2005, pp. 3555-3565.
- [9] Tahani Alsarayreh and Len Zedel, “Quantifying snowfall rates using underwater sound,” Canadian Meteorological and Oceanographic Society, 2011, pp. 61-66.
- [10] S. Murugam, V. Natarajin, and R. Kumar, “Noise model analysis and estimation of effect due to wind driven ambient noise in shallow water,” *International Journal of Oceanography*, 2011, Article ID 950838.

Vita

The author Joseph Kuhner was born in New Orleans, Louisiana. He received his Bachelor's Degree in Mathematics from Saint Mary's College of California in 2004. After six years of professional work, he received his Master of Science from the University of Southern Mississippi in Hydrography. During his professional development through the Naval Oceanographic Office he enrolled in the Graduate Program for Applied Physics at the University of New Orleans. He worked in support of Naval Oceanographic and Meteorological operations while working on his Thesis. This research work was conducted under the supervision of Dr. Juliette loup in 2018.